

THE MOLECULAR CORES IN THE L1287, AFGL 5142, AND IRAS 20126+4104 REGIONS

ROBERT ESTALELLA,¹ RAINER MAUERSBERGER,² JOSÉ M. TORRELLES,^{3,4} GUILLEM ANGLADA,¹
 JOSÉ F. GÓMEZ,^{3,4} ROSARIO LÓPEZ,¹ AND DIRK MUDERS²

Received 1992 August 24; accepted 1993 June 29

ABSTRACT

The NH_3 (J, K) = (1, 1) and (2, 2) line emission was mapped toward three regions with molecular outflows, L1287, AFGL 5142, and IRAS 20126+4104, using the Effelsberg 100 m telescope. Additional C^{18}O ($J = 2 \rightarrow 1$) and CS ($J = 3 \rightarrow 2$) observations of L1287 were carried out with the IRAM 30 m telescope. For the three regions, the high-density molecular core, as traced by the ammonia emission, peaks very close to the position of the proposed powering sources of the outflows. In AFGL 5142 we favor the radio continuum source proposed by Torrelles et al. (1992b) as the powering source of the outflow. The molecular cores best resolved by the telescope beam are elongated in a direction perpendicular to the outflow axis. The clearest elongation is seen in the most collimated outflow, that of L1287. For this source, a remarkable velocity gradient can be seen along the major axis of the high-density condensation, consistent with a rotation of the core. For L1287 and AFGL 5142 we find that the masses of the high-density cores are much higher than the masses of the outflows, indicating that the elongation of the cores cannot be a consequence of the interaction with the molecular outflow and that the cores can play an important role in the large-scale collimation of the bipolar molecular outflows. For all the cores the molecular gas is probably heated by an internal source. In particular, in L1287 we find a local heating of the molecular gas and line broadening toward the position of the ammonia peak, indicating a physical association of the high-density gas with the powering source of the outflow.

Subject headings: ISM: jets and outflows — ISM: molecules —

ISM: individual objects: (L1287, RNO 1B/1C, AFGL 5142, IRAS 20126+4104)

1. INTRODUCTION

Young stellar objects are frequently associated with strong mass outflows, usually traced by high-velocity wings in the spectra of molecules like CO. There is evidence that these outflows start in an early phase of stellar evolution (e.g., Rodríguez 1990; Mezger et al. 1992). The young stellar objects that are powering the outflows are usually embedded in high-density gas traced by molecules like NH_3 or CS. Thus, there is in general a coincidence between the positions of the ammonia peaks and those of the exciting sources of the outflows, at a scale $\lesssim 0.1$ pc (e.g., Torrelles et al. 1983; Anglada et al. 1989). Therefore, at this scale, ammonia observations can be an important tool for constraining the location of the exciting sources, or for discriminating among several exciting source candidates (e.g., in AFGL 5157; Torrelles et al. 1992).

The physical association of powering sources and dense molecular structures is confirmed by the perturbation of the high-density gas that is produced by strong stellar winds and stellar photons from the embedded powering source. Such perturbations can be observed as broadening of lines associated with outflows and local heating of the molecular gas (Myers et al. 1988; Torrelles et al. 1992c). Ammonia is a good tracer of such perturbations, because the kinetic temperature can be

estimated from the observation of the NH_3 (1, 1) and (2, 2) transitions at similar frequencies, and, thus, with the same angular resolution (e.g., Ho & Townes 1983; Takano 1986; Torrelles et al. 1986, 1989, 1992c).

Since a large fraction of molecular outflows is found to have a bipolar morphology (see, e.g., Fukui 1989), it is important to study the physical agent responsible for the observed collimation. In many cases a high-density structure, located close to the center of the outflow and associated with its powering source, is elongated in a direction perpendicular to the axis of the bipolar outflow and may play an important role in its large-scale collimation (e.g., Torrelles et al. 1983, 1992a; see Rodríguez 1989 for a review). The ammonia molecule is especially well suited to study this high-density gas, since several hyperfine components of the NH_3 (1, 1) transition are easily observable, allowing the determination of the physical parameters of the high-density molecular gas. In particular, it is possible to estimate the mass of the high-density condensation, and to study whether it is able to produce the observed collimation of the outflow.

In this work we present single-dish NH_3 (1, 1) and (2, 2) observations, using the Effelsberg 100 m telescope, toward three molecular outflows with a clear bipolar morphology, L1287, AFGL 5142, and IRAS 20126+4104. The high sensitivity and relatively high angular resolution ($40''$) of our observations will contribute to clarifying some problems related to these sources. L1287 is specially interesting, since a double FU Orionis system, RNO 1B/1C (Kenyon et al. 1993), has been proposed as a candidate for the powering source of the outflow. No previous ammonia observations or reliable determination of the physical parameters of the high-density cloud were known for this source. AFGL 5142 was selected because

¹ Departament d'Astronomia i Meteorologia, Universitat de Barcelona, Av. Diagonal 647, E-08028 Barcelona, Spain; and Laboratori d'Astrofísica, Societat Catalana de Física, IEC, Spain.

² Max-Planck-Institut für Radioastronomie, Auf dem Hügel 69, D-53121 Bonn, Germany.

³ Instituto de Astrofísica de Andalucía, CSIC, Apartado Correos 3004, C/ Sancho Panza s/n, E-18080 Granada, Spain. Present address for J. M. T.

⁴ Harvard-Smithsonian Center for Astrophysics, 60 Garden Street, Cambridge, MA 02138. Present address for J. F. G.

two sources were proposed to be driving the outflow: the infrared source AFGL 5142 and a radio continuum source recently reported by Torrelles et al. (1992b). Both sources were engulfed in a high-density molecular core (Verdes-Montenegro et al. 1989; Pastor et al. 1991), but the limited resolution of these previous observations did not allow us to favor one of the sources in terms of its proximity to the high-density peak. IRAS 20126+4104 was the most energetic outflow and the one with the clearest bipolarity in a sample of outflows associated with cold *IRAS* sources (Wilking, Blackwell, & Mundy 1990), and there was no reported observation of high-density gas associated with it. In these three outflows, our ammonia observations improve significantly the knowledge of the morphology, kinematics, and physical conditions of the high-density gas associated with their powering sources.

2. OBSERVATIONS AND RESULTS

2.1. NH_3

The NH_3 (J, K) = (1, 1) and (2, 2) observations were carried out in 1992 February and March with the Effelsberg 100 m telescope of the Max-Planck-Institut für Radioastronomie under good weather conditions. At the observed wavelength of 1.3 cm, the half-power beamwidth of the telescope is $40''$. We used a cryogenically cooled maser receiver with a 1024 channel autocorrelator spectrometer split into two halves of 512 channels each, to allow the simultaneous observation of NH_3 (1, 1) and (2, 2) lines. The total bandwidth of each half was 6.25 MHz, giving a velocity resolution of 0.15 km s^{-1} . We mapped the regions around the proposed powering sources of the outflows by observing the positions of a grid with half-beam spacing between points ($20''$); for IRAS 20126+4104 a full beam spacing was used for the outermost area. From cross-scans through nearby continuum sources the pointing accuracy was estimated to be better than $8''$.

The CLASS and GRAPHIC packages of IRAM were used to reduce, analyze, and display the ammonia data. We detected NH_3 (1, 1) and (2, 2) emission in the three sources observed. In Figure 1 we show the NH_3 (1, 1) and (2, 2) spectra obtained at the position of the emission peak of each source. The line intensities are given in units of main-beam brightness temperature. In Table 1 we give the line parameters obtained. The intrinsic line widths are in the range $1.7\text{--}2.7 \text{ km s}^{-1}$, and the optical depth of the NH_3 (1, 1) main line ranges from 0.5 to 2.2. In Figures 3, 6, and 9 we show our NH_3 (1, 1) and (2, 2) maps, and in Table 2 we give the physical parameters of the high-density cores derived from the ammonia observations. The rotational temperatures obtained are $\sim 21 \text{ K}$, and the masses of the clumps, obtained from the integration of the ammonia column density, are $(2\text{--}3) \times 10^2 M_\odot$.

2.2. C^{18}O and CS

In order to obtain additional information on the L1287 core, we carried out simultaneous C^{18}O ($J = 2 \rightarrow 1$) and CS ($J = 3 \rightarrow 2$) observations of the region with the IRAM 30 m telescope at Pico Veleta in 1992 September. The 2 and 1.3 mm SIS receivers used were very well aligned ($2''\text{--}3''$). We used position switching, with the reference position $1000''$ east of the source position. The pointing uncertainty was estimated to be $\sim 4''$. The half-power beamwidths at the rest frequencies of 219.5604 GHz (C^{18}O) and 146.96904 GHz (CS) are $\sim 13''$ and $\sim 17''$, respectively. For each transition we used half of a $256 \times 100 \text{ kHz}$ filter bank, which gives a velocity resolution of ~ 0.14 and $\sim 0.20 \text{ km s}^{-1}$ for the C^{18}O and the CS, respectively. Spectra were observed on a 15 point raster with $14''/28''$ spacing at a position angle of 135° (along the major axis of the L1287 ammonia condensation; see § 3.1), centered on $\alpha(1950) = 00^{\text{h}}33^{\text{m}}53^{\text{s}}.3$, $\delta(1950) = 63^\circ12'22''$ ($10''$ south of the *IRAS* position; see § 3.1).

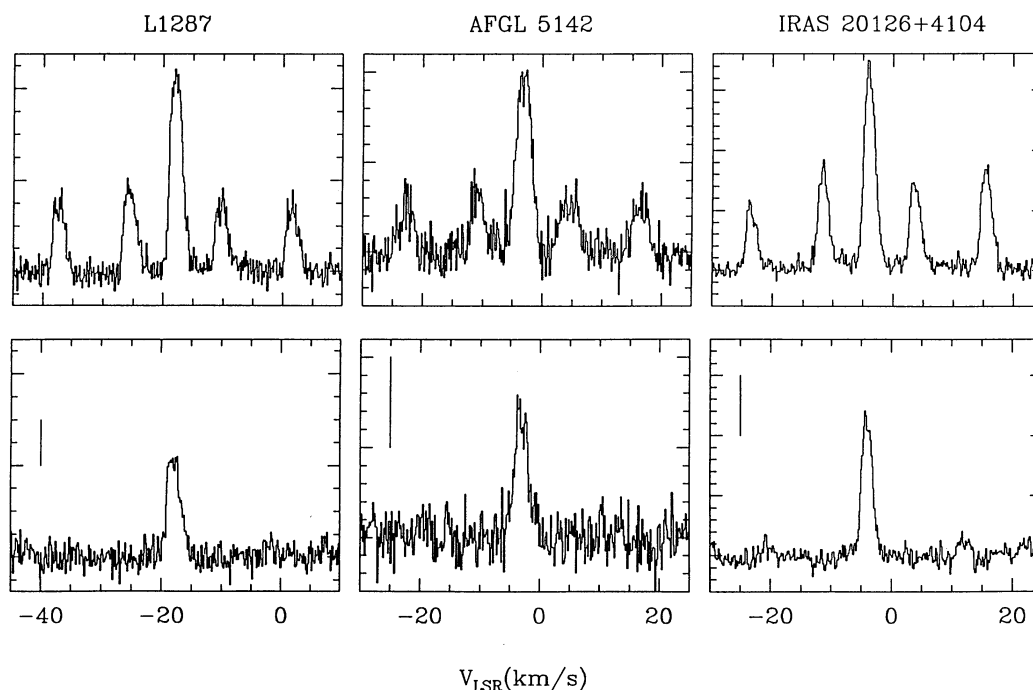


FIG. 1.—Spectra of NH_3 (1, 1) line (top panels) and (2, 2) line (bottom panels) observed at the position of the emission peak in each source. The vertical scale is shown for each source as a vertical bar in the bottom panel, representing 1 K of main-beam brightness temperature.

TABLE 1
NH₃ LINE PARAMETERS^a

Source	Transition (J, K)	V_{LSR} (km s ⁻¹)	$\Delta V_{1/2}^b$ (km s ⁻¹)	τ_m^c	$fT_{\text{ex}}\tau_m^d$ (K)	$N(J, K)^e$ (10 ¹⁴ cm ⁻²)
L1287	(1, 1)	-17.88 ± 0.01	1.93 ± 0.03	1.35 ± 0.10	8.01 ± 0.25	4.4
	(2, 2)	-17.88 ± 0.05	2.34 ± 0.32	0.48 ± 0.18	2.85 ± 1.10	0.9
AFGL 5142	(1, 1)	-3.14 ± 0.03	2.70 ± 0.08	0.50 ± 0.15	2.58 ± 0.14	2.0
	(2, 2)	-3.10 ± 0.06	2.60 ± 0.24	0.30 ± 0.12	1.54 ± 0.41	0.5
IRAS 20126+4104	(1, 1)	-3.96 ± 0.01	1.73 ± 0.02	2.21 ± 0.09	8.02 ± 0.18	4.0
	(2, 2)	-4.01 ± 0.03	1.72 ± 0.09	1.08 ± 0.16	3.91 ± 0.55	0.9

^a Derived from the spectrum at the position of the ammonia peak.

^b Intrinsic line width, taking into account optical depth and hyperfine broadening, but not the spectral resolution of the spectrometer.

^c Optical depth of the main line; for the (1, 1) transition, derived from the relative intensities of the magnetic hyperfine components; for the (2, 2) transition, calculated assuming the same T_{ex} and filling factor f as for the (1, 1) transition.

^d Derived from the transfer equation; f is the filling factor, and T_{ex} is the excitation temperature.

^e Beam-averaged column density for the rotational level (J, K) (Wilson & Mauersberger 1990).

TABLE 2
PHYSICAL PARAMETERS DERIVED FROM THE NH₃ OBSERVATIONS

Source	Distance (kpc)	Angular Size ^a	Linear Size (pc)	Major Axis P.A.	$T_R(22-11)^b$ (K)	$N(\text{H}_2)^c$ (cm ⁻²)	Mass ^d (M_\odot)	Virial Mass ^e (M_\odot)
L1287	0.85	120" × 50"	0.5 × 0.2	135°	20	1.0×10^{23}	210	130
AFGL 5142	1.8	80 × 60	0.7 × 0.5	0	23	4.4×10^{22}	320	460
IRAS 20126+4104	1.7	50 × 40	0.4 × 0.3	10	21	8.9×10^{22}	230	110

^a Deconvolved size of the (1, 1) core, given by $\theta_{\text{deconv}} = [(\theta_{\text{obs}})^2 - (40'')^2]^{1/2}$.

^b Rotational temperature, derived from the column density ratio between the (1, 1) and (2, 2) levels.

^c Hydrogen column density, obtained assuming LTE for the metastable rotational states of NH₃ at $T_k = T_R(22-11)$, and an ammonia abundance $[\text{H}_2/\text{NH}_3] = 10^8$ (Herbst & Klemperer 1973).

^d Derived from the hydrogen column density, assuming a 30% helium-to-hydrogen mass ratio.

^e Obtained from $[M_{\text{virial}}/M_\odot] = 210[R/\text{pc}][\Delta V_{1/2}/\text{km s}^{-1}]^2$, where R is the radius of the source, taken as half the geometrical mean of the two linear sizes, and $\Delta V_{1/2}$ is given in Table 1.

The CLASS and GRAPHIC packages were used to reduce and analyze the C¹⁸O and CS data. In Figure 2 the two series of C¹⁸O ($J = 2 \rightarrow 1$) and CS ($J = 3 \rightarrow 2$) spectra are shown for the velocity range $V_{\text{LSR}} = -26 \text{ km s}^{-1}$ to $V_{\text{LSR}} = -9 \text{ km s}^{-1}$. The line intensities are given in units of main-beam brightness temperature. The CS reaches intensities of up to 11 K and shows double-peaked lines. The central CS spectra exhibit broad wing emission covering almost 10 km s^{-1} . The C¹⁸O spectra have profiles that, for positions symmetrically located with respect to the central position of the raster, are nearly mirror images of each other. Maximum main-beam brightness temperatures are $\sim 5 \text{ K}$. Both lines have full line widths at half-maximum of $\sim 3 \text{ km s}^{-1}$.

We derived an optical depth $\tau(\text{C}^{18}\text{O}) = 0.6$ at the emission peak, assuming LTE conditions and a kinetic temperature equal to the ammonia rotational temperature $T_R(22-11)$ (20 K; Table 2). Using the C¹⁸O data to estimate the spatial extent of the cloud along the major axis and the same ratio of axes as for the ammonia data, and assuming relative abundances $[\text{CO}/\text{C}^{18}\text{O}] = 490$ (terrestrial abundance) and $[\text{H}_2/\text{CO}] = 10^4$ (Herbst & Leung 1989), we estimated a mass of $\sim 70 M_\odot$. Despite the uncertainty in this estimation because of our incomplete mapping of the condensation in C¹⁸O, and the uncertainties in the abundances, this value agrees within a factor of ~ 3 with the mass estimated from ammonia observations ($210 M_\odot$; Table 2).

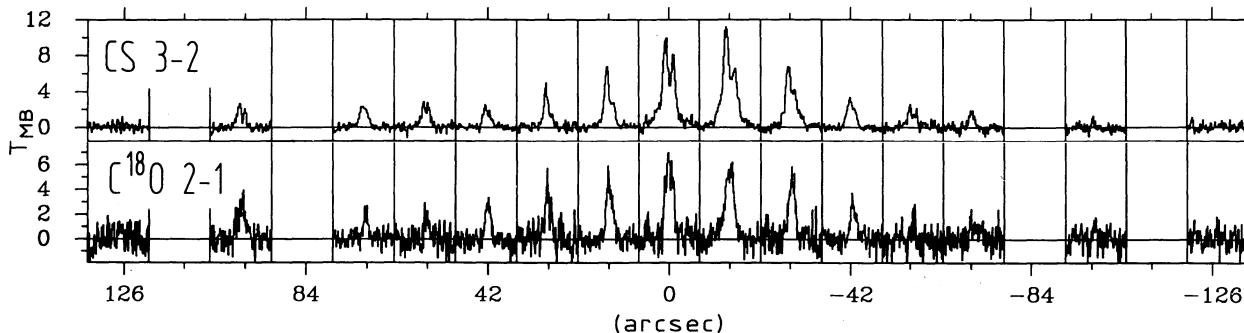


FIG. 2.—Spectra of CS ($J = 3 \rightarrow 2$) and C¹⁸O ($J = 2 \rightarrow 1$) along the major axis of the L1287 NH₃ condensation, at a position angle of 135°, for velocities between $V_{\text{LSR}} = -26 \text{ km s}^{-1}$ and $V_{\text{LSR}} = -9 \text{ km s}^{-1}$. Spacing between neighboring points is 14". The central spectrum corresponds to the position $\alpha(1950) = 00^{\text{h}}33^{\text{m}}53^{\text{s}}.3$, $\delta(1950) = 63^{\circ}12'22''$.

3. INDIVIDUAL SOURCES

3.1. L1287

The main core of the L1287 cloud is part of the globule filament GF 11 (Schneider & Elmegreen 1979). We will adopt a distance of 850 pc for this source (see the discussion in Yang et al. 1991). This cloud includes the cometary nebula GN 00.33.9. This nebula contains two embedded stars, RNO 1B and RNO 1C, separated $\sim 6''$ (~ 5000 AU), which were proposed to constitute a double FU Orionis system (Staude & Neckel 1991; Kenyon et al. 1993). Both stars fall inside the error ellipse of the source IRAS 00338 + 6312.

Snell, Dickman, & Huang (1990) and Yang et al. (1991) mapped in CO an energetic bipolar outflow, with its major axis in the northeast-southwest direction. They associated the outflow with IRAS 00338 + 6312, located close to the outflow center. Kenyon et al. (1993) propose that the system RNO 1B/1C is associated with the IRAS source and is driving the molecular outflow. However, Weintraub & Kastner (1993), on the basis of a polarization study, suggest the existence of a deeply embedded source, some arcseconds northeast of RNO 1B/1C. These authors propose that this embedded source (which they identify with IRAS 00338 + 6312) is the exciting source of the outflow. It is interesting to note that McCutcheon et al. (1991), in a VLA survey, marginally detected 6 cm continuum emission at a level of ~ 0.22 mJy inside the IRAS ellipse error.

The ammonia core as mapped in our $40''$ resolution observations (see Figs. 3 and 4) is clearly elongated in the northwest-southeast direction, perpendicular to the axis of the CO outflow as observed by Snell et al. (1990) and Yang et al. (1991). The size of the ammonia condensation is $\sim 0.5 \times 0.2$ pc (Table 2), in agreement with the size found by Yang et al. (1991) from HCN and HCO^+ observations. The ammonia emission peaks very close (within $\sim 10''$) to the positions of IRAS 00338 + 6312 and RNO 1B/1C (see Fig. 3), which are candidates for the

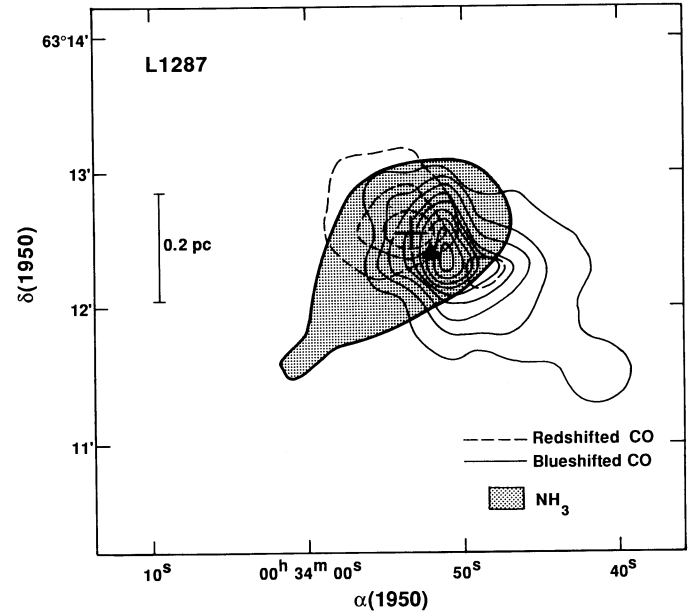


FIG. 4.—High-velocity CO emission in L1287 (Yang et al. 1991) superposed on the NH_3 (1, 1) emission above the half-power level (Fig. 3).

driving source of the molecular outflow (Staude & Neckel 1991; Kenyon et al. 1993; Weintraub & Kastner 1993). The exciting sources of outflows are usually deeply embedded in high-density gas and are found associated with the emission peak of ammonia condensations. This result has been used as a criterion to discriminate among several candidates (e.g., Anglada et al. 1989). However, the separations between the catalog position of the IRAS source and the stars RNO 1B and RNO 1C are only $11''$ and $5''$, respectively, and with our angular resolution we cannot favor either of the sources, in terms of proximity to the ammonia peak. We note that very

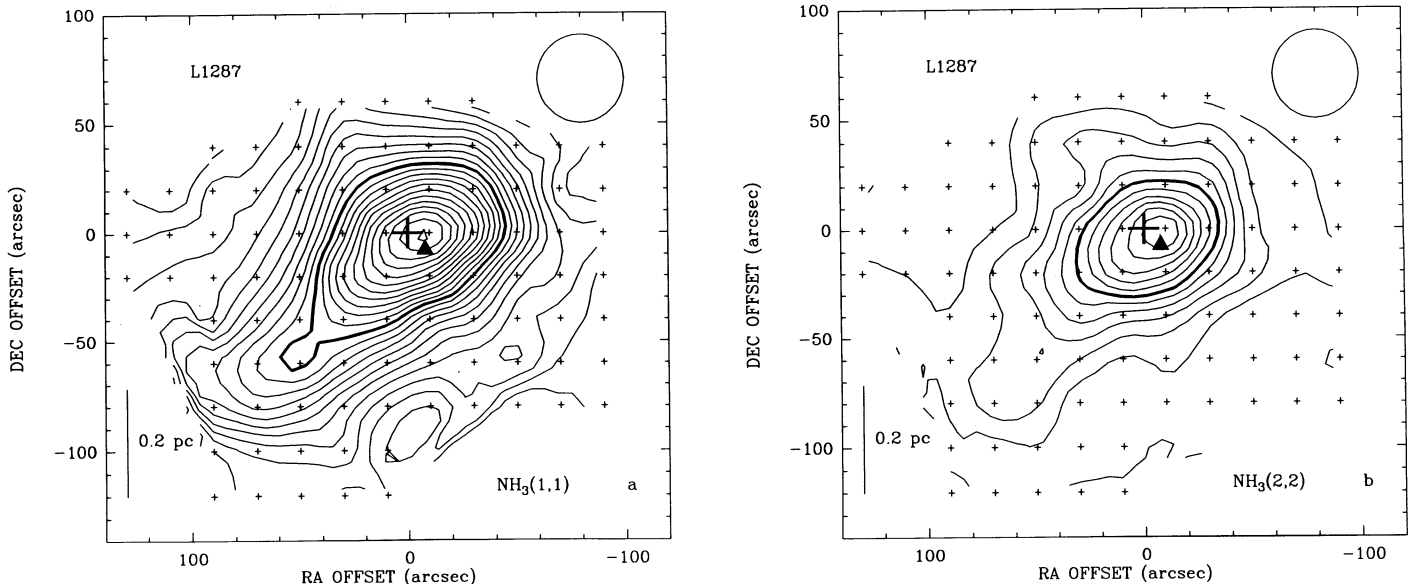


FIG. 3.—(a) Contour map of the integrated line intensity of the NH_3 (1, 1) main line for L1287. The lowest contour level is 0.5 K km s^{-1} , and the increment is 0.5 K km s^{-1} (the thick line indicates the half-power contour). The observed positions are indicated with small plus signs, and the half-power beamwidth is the circle at the upper right. The triangle indicates the position of RNO 1B/1C, and the large plus sign marks the position of IRAS 00338 + 6312. The (0, 0) position is $\alpha(1950) = 00^{\text{h}}33^{\text{m}}53^{\text{s}}.3$, $\delta(1950) = 63^{\circ}12'32''$. (b) Same as (a), but for the NH_3 (2, 2) main line.

recent interferometric observations with high angular resolution ($\sim 7''$; Yang, Ohashi, & Fukui 1993) reveal a peak of CS emission at the catalog position of the *IRAS* source.

In Figure 5 we show the first-order moment (intensity-weighted mean V_{LSR}) of the NH_3 (1, 1) main line. There is a very well defined velocity gradient of $\sim 1.3 \text{ km s}^{-1} \text{ pc}^{-1}$ along the major axis of the condensation. The change in velocity is remarkably smooth along the condensation, the velocity of the southeastern part being $\sim 0.8 \text{ km s}^{-1}$ higher than that of the northwestern part. No velocity gradient in the ammonia lines is observed in the perpendicular direction, i.e., along the axis of the bipolar molecular outflow. If the observed velocity gradient is interpreted as due to the rotation of the high-density condensation, the mass derived for the high-density condensation ($210 M_{\odot}$; Table 2) is large enough to bind this motion gravitationally ($M_{\text{virial}} = 130 M_{\odot}$; Table 2). For an optically thin transition in a rotating core we should expect to observe line profiles that are mirror images of each other for symmetric positions with respect to the center of the map. This is what is observed for the C^{18}O spectra (see Fig. 2). We compared the C^{18}O data with model calculations of rotating ellipsoidal gas clouds (Muders & Schmid-Burgk 1993). Centrally condensed clouds ($\rho \sim r^{-\alpha}$, $2 \leq \alpha \leq 3$) with Keplerian velocity fields fit the data best, although an exact reproduction is not possible. This is probably due to the restriction of the models only to azimuthal motions. C^{18}O observations are thus consistent with rotation of the core. The rotation found in the L1287 core is in agreement with outflow models that predict the existence of a rotating molecular disk (see the discussion in § 4).

The kinematics of the gas traced by the CS ($J = 3 \rightarrow 2$) transition is more complicated. The CS spectra show double-peaked lines, with the blue peak being stronger than the red one (see Fig. 2). This peculiar velocity structure is probably due to self-absorption, since optically thin C^{18}O shows no indication of two components clearly separated in velocity. Similar self-absorption features were observed in HCN, HCO^+ , and

^{12}CO by Yang et al. (1991). There is wing emission in the CS profiles, which is probably associated with outflowing gas, since high-resolution interferometric mapping of CS ($J = 2 \rightarrow 1$) wing emission (Yang et al. 1993) shows the same bipolar pattern as the larger scale CO outflow.

As the NH_3 (1, 1) emission is resolved spatially, it is possible to carry out an analysis of the variation of the rotational temperature and line width along the condensation. As can be seen in Figure 3, the NH_3 (2, 2) emission is more compact than that of the (1, 1) transition. This is indicative of a local heating near the center of the ammonia core. More quantitatively, the rotational temperature at the ammonia peak position is $T_{\text{R}}(22-11) \approx 20 \text{ K}$ (Table 2), while the mean rotational temperature of the observed region, obtained from the average of the observed spectra, is $\sim 15 \text{ K}$. Regarding the NH_3 (1, 1) line widths, the observed line width of the spectra near the position of the ammonia peak is $\sim 2.3 \text{ km s}^{-1}$, which is $\sim 0.5 \text{ km s}^{-1}$ larger than the line width of the average of the observed spectra. The observed local heating and line broadening at the position of IRAS 00338 + 6312 and RNO 1B/1C implies a physical association of the high-density gas with one or more of these sources. Ammonia observations with higher angular resolution could discriminate between the different sources proposed to be driving the L1287 outflow. In addition, as the exciting sources of outflows are commonly found to have associated radio continuum emission (e.g., Anglada et al. 1992), high-resolution radio continuum observations could help to identify the exciting source of the L1287 outflow.

3.2. AFGL 5142

The very red embedded object AFGL 5142 (IRAS 05274 + 3345) is located in the Perseus arm, at a distance of 1.8 kpc (Snell et al. 1988). Optical and near-infrared observations carried out by Eiroa et al. (1993) reveal the presence of a small stellar cluster surrounded by a diffuse nebula. The *IRAS* source appears to coincide with one of these stars, which is associated with a cometary nebula.

A bipolar CO outflow, whose geometrical center is located toward the *IRAS* position, was reported by Snell et al. (1988). The high-density gas toward this region was mapped through the emission of NH_3 (Verdes-Montenegro et al. 1989) and CS (Pastor et al. 1991). The high-density condensation, barely resolved by the telescope beams in those observations ($\sim 1.5''$), engulfed the *IRAS* source, proposed as the powering source of the outflow. Verdes-Montenegro et al. (1989) detected an H_2O maser inside the ammonia clump, displaced $\sim 50''$ from the catalog position of the *IRAS* source. More recently, Torrelles et al. (1992b), through VLA observations, refined the position of the water maser and found a 3.6 cm continuum source coinciding within $2''$ with the maser. Torrelles et al. (1992b) suggested that the radio continuum source could be excited by a B2 zero-age main-sequence (ZAMS) star. Thus, two sources related to early-type stars that may be undergoing mass loss (IRAS 05274 + 3345 and the VLA radio continuum source) are located close to the center of the molecular outflow, inside the high-density clump, and can contribute to powering the outflow.

The ammonia core as mapped in our 100 m observations (see Figs. 6 and 7) is slightly elongated ($80'' \times 60''$) in the north-south direction, perpendicular to the outflow axis as mapped by Snell et al. (1988). The peak of the ammonia condensation nearly coincides (within $\sim 10''$) with the radio continuum

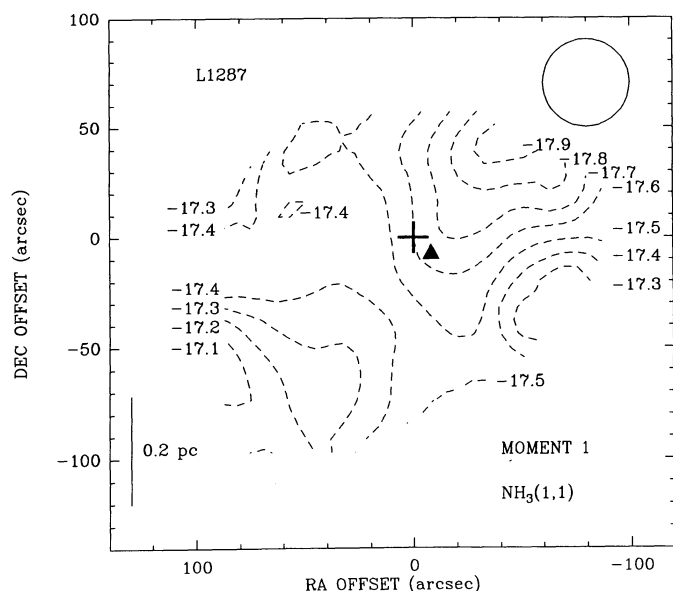


FIG. 5.—Contour map of the first-order moment (intensity-weighted mean V_{LSR}) of the NH_3 (1, 1) main line for L1287. The V_{LSR} corresponding to each contour level is indicated in the figure. Note the very well defined gradient in velocity in the northwest-southeast direction.

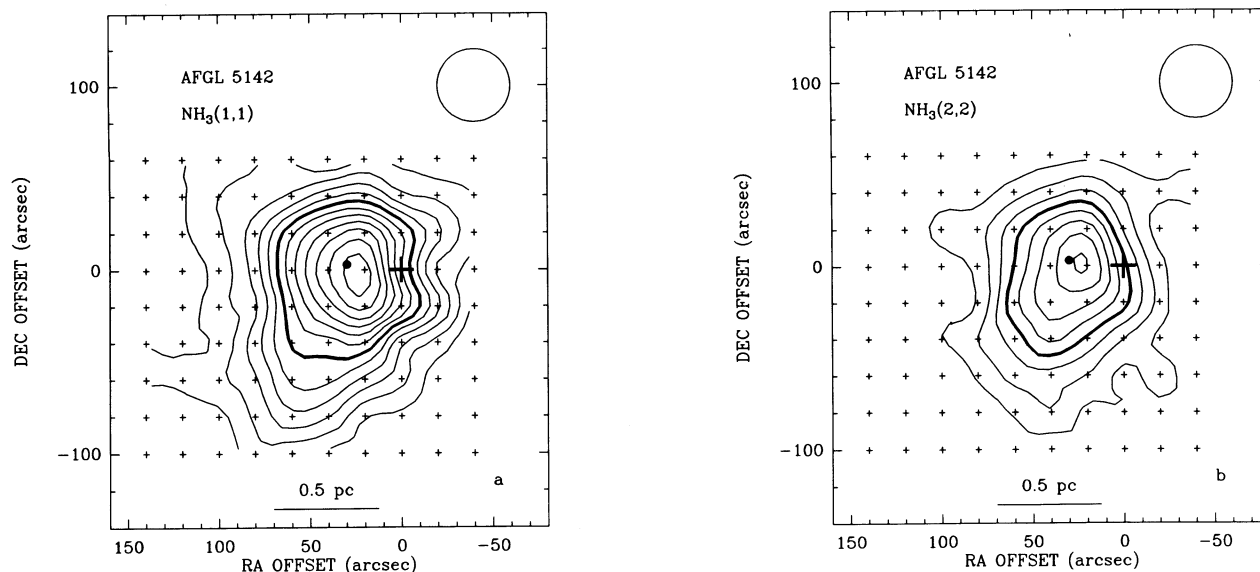


FIG. 6.—Same as Fig. 3, but for AFGL 5142. The lowest contour level is 0.5 K km s^{-1} , and the increment is 0.5 K km s^{-1} . The filled circle indicates the position of the radio continuum source (Torrelles et al. 1992b), and the large plus sign marks the position of IRAS 05274+3345. The (0,0) position is $\alpha(1950) = 05^{\text{h}}27^{\text{m}}27^{\text{s}}.6$, $\delta(1950) = 33^{\circ}45'37''$.

source detected by Torrelles et al. (1992b), while the *IRAS* source lies close to the half-intensity contour of the condensation (see Fig. 6). As the peak of high-density clumps is usually found associated with the exciting sources of outflows, our results suggest that the AFGL 5142 outflow is powered by the object that is ionizing the VLA radio continuum source.

In Figure 8 we show position-velocity plots through $\Delta\alpha = 20''$ and through $\Delta\delta = 0''$ for the NH_3 (1,1) main line. Two velocity components can be distinguished: one with a velocity of $\sim -3.7 \text{ km s}^{-1}$ (which shows a small velocity gradient of $\sim 0.5 \text{ km s}^{-1} \text{ pc}^{-1}$ in the north-south direction; see Fig. 8a), and another with a velocity of $\sim -2.7 \text{ km s}^{-1}$. Both velocity components appear also in the NH_3 (2,2) line. The

component at -2.7 km s^{-1} peaks at the position of the radio continuum source.

The rotational temperature obtained from the ratio of the NH_3 (1,1) and (2,2) lines at the ammonia peak position is 23 K (Table 2). This temperature is higher than the values derived for other cores of dark clouds ($\sim 10 \text{ K}$; see § 4). Therefore, an internal heating source is probably present in AFGL 5142, associated with the radio continuum source and the H_2O maser found in the region. Unfortunately, we do not have enough angular resolution to measure a local heating at this position.

3.3. IRAS 20126+4104

This region is located in Cygnus X, at an estimated distance of 1.7 kpc (Dame & Thaddeus 1985). High-velocity CO emission was detected and mapped by Wilking et al. (1989, 1990) in a survey of cold *IRAS* sources. The outflow presented the highest velocity gas (full velocity width $\approx 63 \text{ km s}^{-1}$), momentum rate, and mechanical luminosity of the sample. The molecular outflow shows a very clear bipolar morphology, with its axis in the north-south direction, although with a low collimation. The proposed powering source, IRAS 20126+4104, is located at the center of the outflow. The estimated far-infrared luminosity of the source is $\sim 1.8 \times 10^4 L_{\odot}$, which is consistent with an embedded B0 ZAMS star (Walker, Adams, & Lada 1990).

The ammonia core as mapped in our $40''$ resolution observations (see Figs. 9 and 10) is well centered on the molecular outflow, with the emission peak coinciding (within $\sim 5''$) with the *IRAS* source (see Fig. 9). No significant elongation of the high-density core is seen from our data, probably because of the limited angular resolution. However, a velocity shift of $\sim 1 \text{ km s}^{-1}$ can be seen from the NH_3 (1,1) and (2,2) data, with the velocity increasing from south to north (see Fig. 11). Since the core is only marginally resolved by our observations, we cannot study the distribution of the velocity field in this core, as has been done in the L1287 core (see § 3.1). Therefore, our

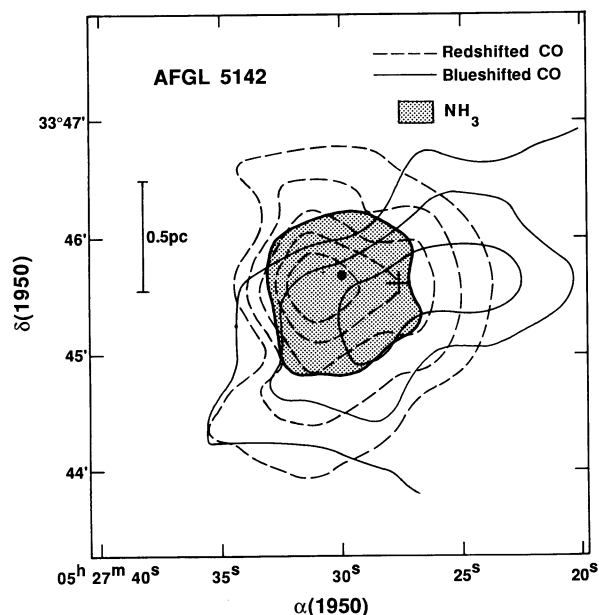


FIG. 7.—High-velocity CO emission in AFGL 5142 (Snell et al. 1988) superposed on the NH_3 (1,1) emission above the half-power level (Fig. 6).

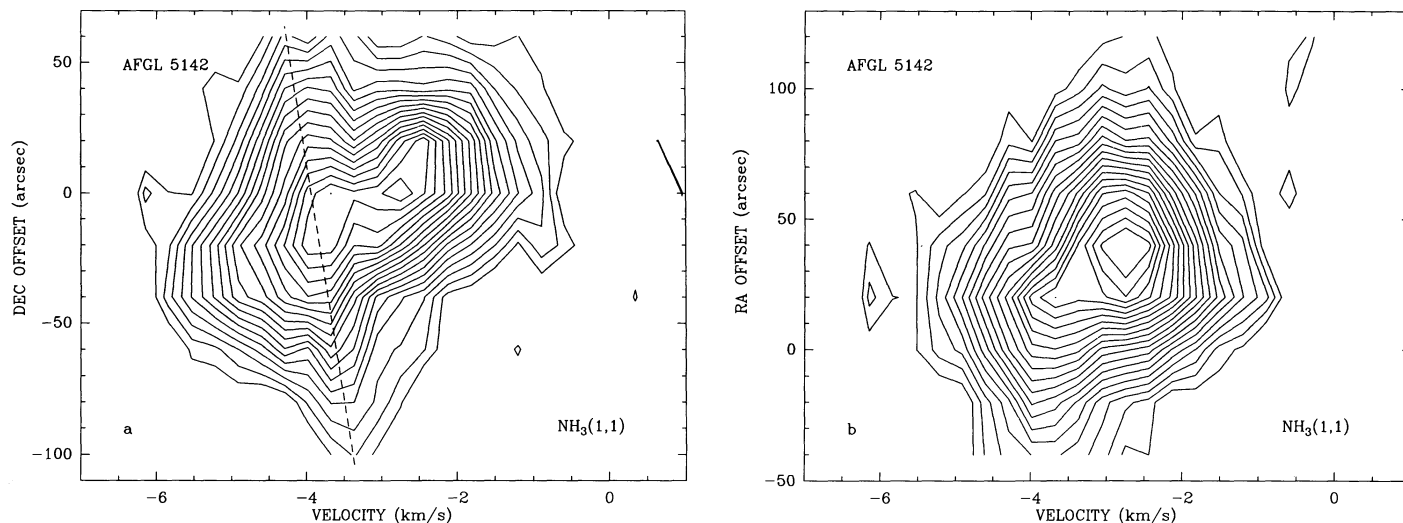


FIG. 8.—Position-velocity plot (a) through $\Delta\alpha = 20''$ and (b) through $\Delta\delta = 0''$ for the $\text{NH}_3(1,1)$ main line for AFGL 5142. The lowest contour level is 0.2 K, and the increment is 0.1 K. Two velocity components can be seen, the first with a velocity of $\sim -3.7 \text{ km s}^{-1}$ and the second with a velocity of $\sim -2.7 \text{ km s}^{-1}$. The dashed line in (a) indicates the small velocity gradient of the first velocity component.

data do not allow a complete discussion of the origin of the observed velocity shift. We can probably discard the interpretation of the velocity shift as rotation of a molecular disk, since the shift is along the direction of the outflow axis. Neither can it be explained by high-density gas dragged by the outflow, because this velocity shift of the ambient molecular gas is of opposite sign as compared with the high-velocity gas. However, we think that this shift is real, since it is consistent with that reported by Wilking et al. (1990) in the velocity of the ambient cloud as traced by the CO emission. Further studies with higher angular resolution would give important clues about the origin of this velocity shift.

The *IRAS* source is associated with a large mass of cold dust and gas. The millimeter continuum emission from the dust associated with the *IRAS* source was observed by Wilking et

al. (1989) at 2.7 mm and by Walker et al. (1990) at 1.3 mm. The masses estimated from the dust observations are $\sim 40 M_\odot$. Dust mass determinations are heavily affected by the choice of the dust opacity law (André, Ward-Thompson, & Barsony 1993), while the mass derived from the ammonia emission ($230 M_\odot$; Table 2) depends on the ammonia abundance adopted. Despite these uncertainties, both values agree within a factor of 2–3 with the virial mass ($110 M_\odot$; Table 2).

The rotational temperature obtained from the $\text{NH}_3(1,1)$ and (2,2) lines at the ammonia peak position is 21 K (Table 2). As in the case of AFGL 5142, the temperature obtained is higher than the values derived for other cores of dark clouds. Therefore, we suggest that the *IRAS* source is physically associated with the high-density clump and is heating the molecular gas of the core. However, temperature gradients

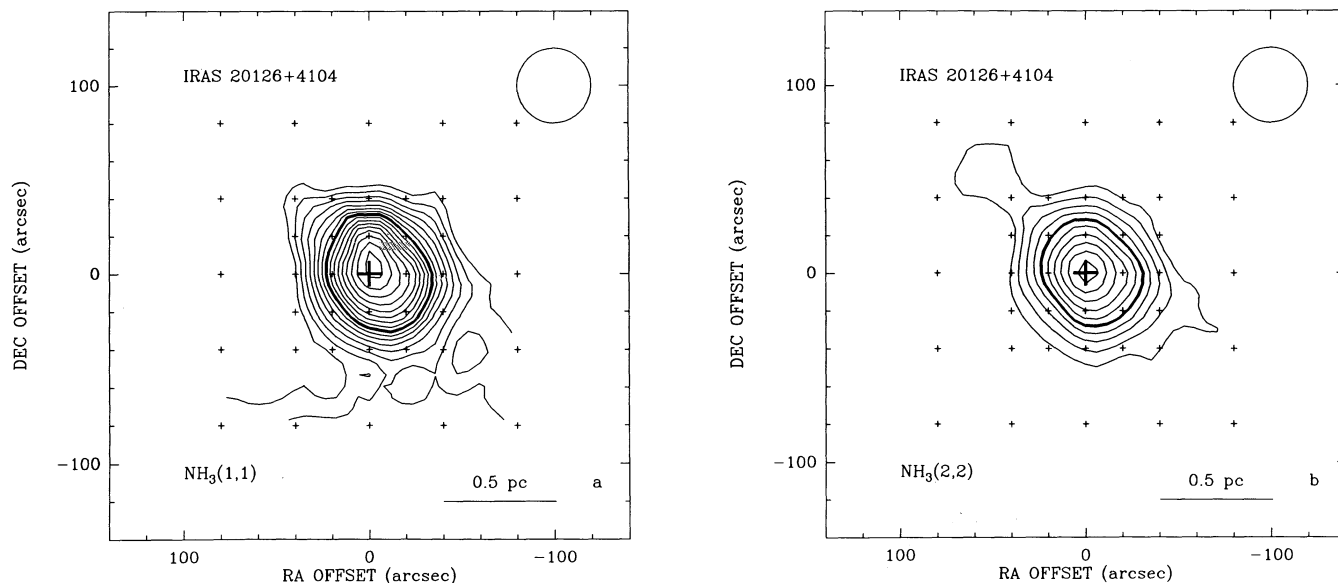


FIG. 9.—Same as Fig. 3, but for IRAS 20126+4104. The lowest contour level is 0.5 K km s^{-1} , and the increment is 0.5 K km s^{-1} . The large plus sign marks the position of the *IRAS* source. The (0,0) position is $\alpha(1950) = 20^{\text{h}}12^{\text{m}}41^{\text{s}}.0$, $\delta(1950) = 41^{\circ}04'20''$.

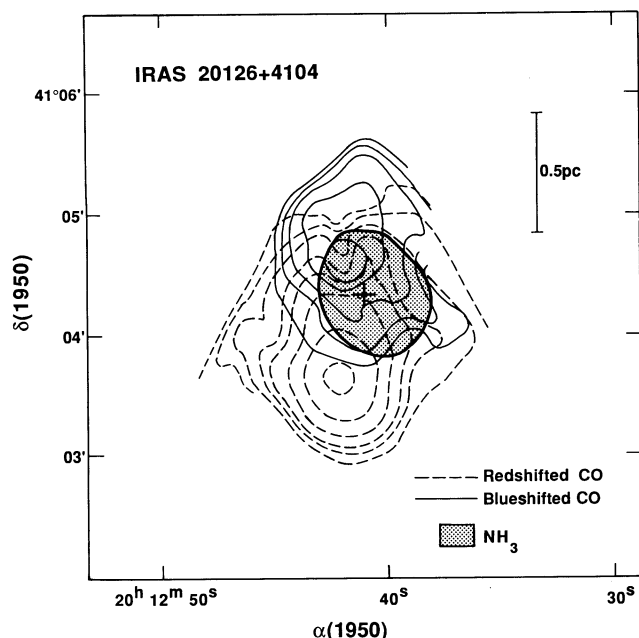


FIG. 10.—High-velocity CO emission in IRAS 20126+4104 (Wilking et al. 1990) superposed on the NH_3 (1, 1) emission above the half-power level (Fig. 9).

toward the position of the *IRAS* source cannot be measured from our data, probably because of our limited angular resolution.

4. GENERAL DISCUSSION AND CONCLUSIONS

Bipolar molecular outflows require a mechanism responsible for the observed collimation. Several models show that an originally isotropic stellar wind can be collimated by a surrounding flattened structure and originate the molecular outflow (Barral & Cantó 1981; Königl 1982; Hanani & Sakashita 1987). Even if the stellar wind is not originally isotropic, magnetohydrodynamic models for bipolar outflows require a molecular disk whose rotational energy is released as a bipolar wind (Pudritz & Norman 1983; Uchida & Shibata 1985; Pudritz 1988). For the three bipolar outflows studied in this

paper, we detected the predicted high-density structures at the center of the outflows. The ammonia condensations have sizes of the order of 0.5 pc, a value similar to that found by Anglada et al. (1989) and Benson & Myers (1989) for cores with embedded sources. The molecular cores best resolved by our beam, L1287 and AFGL 5142, are elongated in a direction perpendicular to the molecular outflow axes, as expected from models for bipolar outflows. The clearest elongation is seen in the best-collimated outflow, L1287. For this source, the NH_3 and C^{18}O data are consistent with the rotation of the high-density core.

For the three sources, the high-density molecular core, as traced by the ammonia emission, peaks near the position of young stellar objects which have been proposed as powering sources of the outflows. This result confirms that, in general, ammonia peaks coincide with outflow exciting sources (e.g., Torrelles et al. 1983; Anglada et al. 1989). In addition, in AFGL 5142 our observations discriminate among two candidates, and favor the object associated with the VLA radio continuum source reported by Torrelles et al. (1992b).

The values obtained for the mass of the high-density cores agree within a factor of ~ 2 with the virial mass of each condensation (Table 2). The mass for L1287 estimated from the C^{18}O data is compatible with the value obtained from NH_3 . This is an indication that the abundance adopted for the ammonia molecule, $[\text{H}_2/\text{NH}_3] = 10^8$ (Herbst & Klemperer 1973), is adequate for these sources.

The masses of the molecular outflows in the three regions, L1287, AFGL 5142, and IRAS 20126+4104, are $0.3\text{--}2.5 M_\odot$ (Yang et al. 1991; Snell et al. 1990), $\sim 5 M_\odot$ (Snell et al. 1988), and $\sim 67 M_\odot$ (Wilking et al. 1990), respectively. For L1287 and AFGL 5142, the masses of the high-density cores are much higher than the mass of the corresponding molecular outflow. This result indicates that the elongation of the cores in L1287 and AFGL 5142 is not the consequence of the action of the bipolar outflow, which would have cleared the high-density gas along the direction of the outflow. Thus the elongation precedes the outflow phase, as was pointed out by Rodríguez (1989) and by Torrelles et al. (1992a) for other star-forming regions. This result is in agreement with the conclusion of Myers et al. (1991), who, from a study of elongation in high-density cores with and without stars, concluded that elongation is a condition prior to star formation. Therefore, we conclude that the elongated molecular cores in L1287 and AFGL 5142 existed before the outflow phase started and that they can play an important role in the large-scale collimation of the bipolar molecular outflow, even if the stellar wind is already collimated at much smaller scales.

Multitransition ammonia observations provide a unique tool for study of the perturbation of the high-density gas by the powering source of the outflow, since the rotational temperature, a good estimator of the kinematic temperature of the gas, can be easily obtained from observations with the same angular resolution. The rotational temperature at the ammonia peak position for the three sources is 20–23 K (Table 2). These values of the rotational temperature correspond to kinetic temperatures of 25–30 K (Walmsley & Ungerechts 1983). This temperature is higher than the values derived for other cores of dark clouds (~ 10 K) where the main heating mechanism is cosmic rays (Goldsmith & Langer 1978). Therefore, an internal heating source is probably present in the three sources. This heating of the cores confirms the association of the observed high-density gas with the exciting sources of the

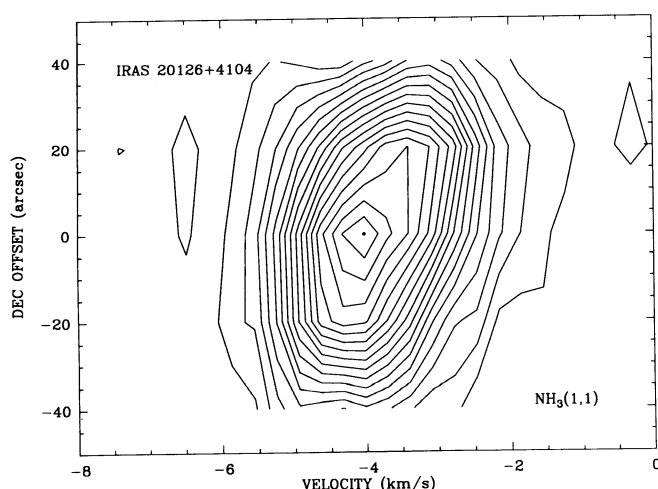


FIG. 11.—Position-velocity plot through $\Delta\alpha = 0''$ for the NH_3 (1, 1) main line for IRAS 20126+4104. The lowest contour level is 0.2 K, and the increment is 0.2 K.

outflows. In particular, in L1287 we have been able to measure a local heating toward the center of the ammonia core. Since in this source several candidates separated $\sim 10''$ have been proposed as the outflow exciting source, we think that VLA ammonia observations (resolution $\leq 4''$) will certainly be very valuable in order to identify the source associated with the perturbation of the high-density gas, as has been done in other regions (e.g., Serpens: Torrelles et al. 1992c; Cepheus A: Torrelles et al. 1993). The results obtained in this paper show the usefulness of single-dish ammonia observations to probe the physical conditions of the high-density gas associated with outflow regions. These observations are an important and

necessary step in the study, with increasing sensitivity and resolution, of the interaction of the molecular outflows with their high-density environment.

G. A. and R. E. acknowledge the hospitality of the Harvard-Smithsonian Center for Astrophysics during the preparation of the paper. G. A. acknowledges support from an Henri Chrétien award administered by the American Astronomical Society. J. F. G. acknowledges support from a Smithsonian predoctoral fellowship. This work has been partially supported by DGICYT grants PB87-0371 and PB92-0900 (Spain).

REFERENCES

- André, P., Ward-Thompson, D., & Barsony, M. 1993, *ApJ*, 406, 122
 Anglada, G., Rodríguez, L. F., Cantó, J., Estalella, R., & Torrelles, J. M. 1992, *ApJ*, 395, 494
 Anglada, G., Rodríguez, L. F., Torrelles, J. M., Estalella, R., Ho, P. T. P., Cantó, J., López, R., & Verdes-Montenegro, L. 1989, *ApJ*, 341, 208
 Barral, J. F., & Cantó, J. 1981, *Rev. Mexicana Astron. Af.*, 5, 101
 Benson, P. J., & Myers, P. C. 1989, *ApJS*, 71, 89
 Dame, T. M., & Thaddeus, P. 1985, *ApJ*, 297, 751
 Eiroa, C., Anglada, G., Estalella, R., Miranda, L. F., & Torrelles, J. M. 1993, *A&AS*, submitted
 Fukui, Y. 1989, in *ESO Workshop on Low Mass Star Formation and Pre-Main-Sequence Objects*, ed. B. Reipurth (Garching: ESO), 95
 Goldsmith, P. G., & Langer, W. D. 1978, *ApJ*, 278, 156
 Hanani, H., & Sakashita, S. 1987, in *IAU Symp. 115, Star Forming Regions*, ed. M. Peimbert & J. Jugaku (Dordrecht: Reidel), 391
 Herbst, E., & Klemperer, W. 1973, *ApJ*, 185, 505
 Herbst, E., & Leung, C. M. 1989, *ApJS*, 69, 271
 Ho, P. T. P., & Townes, C. H. 1983, *ARA&A*, 21, 239
 Kenyon, S. J., Hartmann, L., Gómez, M., Carr, J. S., & Tokunaga, A. 1993, *AJ*, 105, 1505
 Königl, A. 1982, *ApJ*, 261, 115
 McCutcheon, W. H., Dewdney, P. E., Purton, C. R., & Sato, T. 1991, *AJ*, 101, 1435
 Mezger, P. G., Sievers, A. W., Haslam, C. G. T., Kreysa, E., Lemke, R., Mauersberger, R., & Wilson, T. L. 1992, *A&A*, 256, 631
 Muders, D., & Schmid-Burgk, J. 1993, in preparation
 Myers, P. C., Fuller, G. A., Goodman, A. A., & Benson, P. J. 1991, *ApJ*, 376, 561
 Myers, P. C., Heyer, M. H., Snell, R. L., & Goldsmith, P. F. 1988, *ApJ*, 324, 907
 Pastor, J., Estalella, R., López, R., Anglada, G., Planesas, P., & Buj, J. 1991, *A&A*, 252, 320
 Pudritz, R. E. 1988, in *Galactic and Extragalactic Star Formation*, ed. R. E. Pudritz & M. Fich (Dordrecht: Kluwer), 135
 Pudritz, R. E., & Norman, C. A. 1983, *ApJ*, 274, 677
 Rodríguez, L. F. 1989, in *IAU Colloq. 120, Structure and Dynamics of the Interstellar Medium*, ed. M. Moles & T. Tagle (Berlin: Springer), 197
 Rodríguez, L. F. 1990, in *ASP Conf. Ser. 12, Evolution of the Interstellar Medium*, ed. L. Blitz (San Francisco: ASP), 183
 Schneider, S., & Elmegreen, B. G. 1979, *ApJS*, 41, 87
 Snell, R. L., Dickman, R. L., & Huang, Y. L. 1990, *ApJ*, 352, 139
 Snell, R. L., Huang, Y. L., Dickman, R. L., & Claussen, M. J. 1988, *ApJ*, 325, 853
 Staude, H. J., & Neckel, Th. 1991, *A&A*, 244, L16
 Takano, T. 1986, *ApJ*, 303, 349
 Torrelles, J. M., Eiroa, C., Mauersberger, R., Estalella, R., Miranda, L. F., & Anglada, G. 1992a, *ApJ*, 384, 528
 Torrelles, J. M., Gómez, J. F., Anglada, G., Estalella, R., Mauersberger, R., & Eiroa, C. 1992b, *ApJ*, 392, 616
 Torrelles, J. M., Gómez, J. F., Curiel, S., Eiroa, C., Rodríguez, L. F., & Ho, P. T. P. 1992c, *ApJ*, 384, L59
 Torrelles, J. M., Ho, P. T. P., Rodríguez, L. F., & Cantó, J. 1986, *ApJ*, 305, 721
 ———, 1989, *ApJ*, 343, 222
 Torrelles, J. M., Rodríguez, L. F., Cantó, J., Carral, P., Marcaide, J., Moran, J., & Ho, P. T. P. 1983, *ApJ*, 274, 214
 Torrelles, J. M., Verdes-Montenegro, L., Ho, P. T. P., Rodríguez, L. F., & Cantó, J. 1993, *ApJ*, 410, 202
 Uchida, Y., & Shibata, K. 1985, *PASJ*, 37, 515
 Verdes-Montenegro, L., Torrelles, J. M., Rodríguez, L. F., Anglada, G., López, R., Estalella, R., Cantó, J., & Ho, P. T. P. 1989, *ApJ*, 346, 193
 Walker, C. K., Adams, F. C., & Lada, C. J. 1990, *ApJ*, 349, 515
 Walmsley, C. M., & Ungerechts, H. 1983, *A&A*, 122, 164
 Weintraub, D. A., & Kastner, J. 1993, *ApJ*, 411, 767
 Wilking, B. A., Blackwell, J. H., & Mundy, L. G. 1990, *AJ*, 100, 758
 Wilking, B. A., Mundy, L. G., Blackwell, J. H., & Howe, J. E. 1989, *ApJ*, 345, 257
 Wilson, T. L., & Mauersberger, R. 1990, *A&A*, 239, 305
 Yang, J., Ohashi, N., & Fukui, Y. 1993, in *Second Northeast-Asian Regional Meeting on Recent Development in Millimeter-Wave and Infrared Astronomy* (Daejeon), in press
 Yang, J., Umemoto, T., Iwata, T., & Fukui, Y. 1991, *ApJ*, 373, 137

Note added in proof.—Recently, Anglada et al. (*ApJ*, submitted [1993]) detected with the VLA a centimeter radio continuum source in L1287 coincident within $1''$ with the position of the embedded object predicted by Weintraub & Kastner (1993). The radio source is marginally elongated along the axis of the bipolar outflow, suggesting that this object is a radio jet associated with the exciting source of the L1287 outflow.